Available online at www.sciencedirect.com
SCIENCE DIRECT®
Advances in Space Research 34 (2004) 573–577
ADVANCES IN SPACE RESEARCH (a COSPAR publication)
www.elsevier.com/locate/asr

ASTRO-F/FIS observing simulation including detector characteristics

Woong-Seob Jeong [a,*], Soojong Pak [a,b], Hyung Mok Lee [a], Takao Nakagawa [c], Minjin Kim [a], Sang Hoon Oh [a], Hidehiro Kaneda [c], Sin'itirou Makiuti [c], Mai Shirahata [c], Shuji Matsuura [c], Mikhail A. Patrashin [c], Chris Pearson [d], Hiroshi Shibai [e]

[a] *Graduate School of Earth and Environmental Sciences, Seoul National University, Shillim-Dong, Kwanak-Gu, Seoul 151-742, Republic of Korea*
[b] *Korea Astronomy Observatory, Whaam-Dong, Yuseong-Gu, Taejeon 305-348, Republic of Korea*
[c] *Institute of Space and Astronautical Science, Yoshinodai 3-1-1, Sagamihara, Kanagawa 229-8510, Japan*
[d] *Astrophysics Group, Imperial College of Science Technology and Medicine, London SW7 2BZ, UK*
[e] *Graduate School of Science, Nagoya University Furo-cho, Chigusa-ku, Nagoya 464-8602, Japan*

Received 21 February 2003; received in revised form 10 April 2003; accepted 15 April 2003

Abstract

We have examined the effects of transients, glitches caused by cosmic ray hits, and the crosstalk of the far-infrared detector arrays on-board ASTRO-F on its survey mode data. We used simple model fits to laboratory measurements for the transients and glitch profiles. We also tested several correction methods, based on these models, to recover the original signal.

Keywords: ASTRO-F; Far-infrared surveyor; Data analysis; Observing simulation; Detector characteristics

1. Introduction

ASTRO-F is the next generation infrared space telescope of the Japanese Institute of Space and Astronautical Science due for launch in 2005. One of its instruments, the far-infrared surveyor (FIS) will map the entire sky in four bands using short wavelength (SW) and long wavelength (LW) detector arrays (Murakami, 1998; Shibai, 2000; Nakagawa, 2001). We have developed a suite of software with an aim to simulate the FIS observations (Jeong et al., 2000, 2003, 2004). Such software will be used for many different purposes: e.g., to check the hardware performance for realistic sources, to design the optimal observational modes, and to generate virtual data that can be used in constructing the data reduction software.

The FIS uses two Ge:Ga arrays: unstressed for SW and stressed for LW. It is well known that these arrays exhibit many non-ideal characteristics such as a slow transient response, non-linear crosstalk among detector pixels, and susceptibility to high energy radiation (Matsuura et al., 2003). The correction of these effects is essential for the data reduction process. We can examine the consequences of such complex effects by using our simulation software. In this paper, we present results of simulations that include glitches by cosmic rays, detector transients, and crosstalk between adjacent detector pixels. The simulated raw data show how serious these effects could be on the real observations. By carefully analysing the simulated data, we suggest appropriate methods to remove such effects.

2. Detector response

Ideally, the detector should record the incoming signal instantaneously with a steady responsivity and there should be no interference from nearby pixels. However in practice, the anomalous behavior of a detector and unstable conditions of space environment cause changes in the detector response.

* Corresponding author. Tel.: +82-2-880-6776; fax: +82-2-887-1435.
E-mail address: jeongws@astro.snu.ac.kr (W.-S. Jeong).

0273-1177/$30 © 2004 COSPAR. Published by Elsevier Ltd. All rights reserved.
doi:10.1016/j.asr.2003.04.043

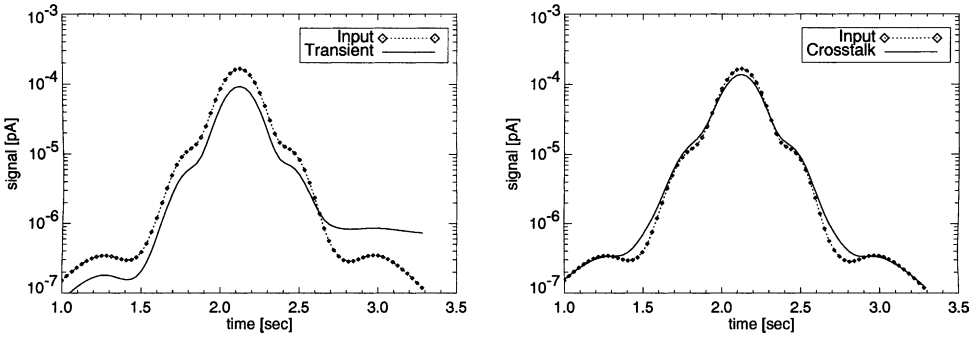

Fig. 1. Profiles of the point source in simulated scans measured by an ideal detector and detectors exhibiting the slow transient response (left panel), and the crosstalk due to lateral diffusion (right panel).

Since the detectors do not respond instantaneously to an incoming signal (e.g., photon), the output signal has different shape from the input in the scanning data. This is known as the transient behavior of the detector. The right panel of Fig. 1 shows clearly that the transient shifts the peak in time, lowers the peak, and produces a long tail after the peak. The transient is usually characterized by a time constant, but this constant can in fact vary with the strength of input signal.

A small fraction of the charge carriers, generated in a particular detector by the incident photons, could leak into neighboring pixels due to lateral diffusion (Rieke, 1994). This is the simplest type of the stationary crosstalk which results in a blurring of the signal as shown in the right panel of Fig. 1. The crosstalk does not change the position of the peak but it makes the peak lower and point spread function (PSF) wider.

In orbit, high energy particles often hit the detectors producing glitches in the time series data. After a cosmic ray hit, the responsivity of a detector becomes much higher than the nominal value for an extended period. We consider these three effects: transients, crosstalk, and glitches in the observing simulations of ASTRO-F/FIS, based on the laboratory measurements of these effects. Note, we have not taken into account the change of responsivity after a cosmic ray hit because we require more laboratory data to model this effect.

3. Modeling of detector response

In order to simulate the detector response, it is useful to model the laboratory data by simple functions.

3.1. Transients

The laboratory data for transients (and also its after effect: see below) can be represented by several different models: examples being a one- or two-component Lari model (Lari et al., 2001), or a one- or two-component exponential model. Although these models have quite different functional forms, the differences in the model response are very small. Therefore, we employed the two-component exponential model which has the following simple form for the response function, $r(t)$

$$r(t) = \left(1 - \sum_{i=1}^{2} B_i\right)\delta(t - t_0) + \sum_{i=1}^{2}\left\{\frac{B_i}{\tau_i}\exp\left[-\frac{t - t_0}{\tau_i}\right]\right\}, \quad (1)$$

where $\delta(t)$ is a delta function, t is the time, τ is the time constant, and B is the contribution of the transient component. The detector readout is an integration of $r(t)$ times the input signal $f(t)$ from t_0 to t. Thus the readout at t can be computed from $R(t) = \int_0^t f(t-u)r(u)\,\mathrm{d}u$, where $u = t - t_0$ and $u \geqslant 0$. The four parameters in Eq. (1) are listed in Table 1. The time constants and the "contribution constants" depend on the amount of photocurrent through the detector.

3.2. Stationary crosstalk

We model the crosstalk in the simulation by transferring some fraction of the integrated charge to nearby pixels. Based on laboratory data, we assume a response where 20% of the pixel value goes to adjacent pixels and 5% goes to nearby pixels in diagonal direction in the SW bands. For the LW bands, 5% goes to adjacent pixels and 1% goes to diagonal pixels (Matsuura et al., 2003). The crosstalk causes the full width at half maximum (FWHM) of the image to increase by 15% in the SW bands and 5% in the LW bands, respectively. Since we also apply this crosstalk response to the marginal pixels, i.e., a pixel located at the end of a row or column, this gives some amount of flux to the surrounding eight

Table 1
Time-constants and contributions of transient component (Kaneda et al., 2002)

Parameters	Time-constant (τ) (s)	Contribution of transient component (B) (pA)
τ_1, B_1	$9.0 \times J^{-0.79}$	$0.154 \times J^{0.06}$
τ_2, B_2	$1.11 \times J^{-0.35}$	$0.177 \times J^{-0.08}$

J, photocurrent (pA).

pixels including empty pixels, therefore, will be a loss of flux of ~10% in the SW bands and ~3% in the LW bands, respectively.

3.3. Glitches

From an extensive analysis of glitches with various models (Kim et al., 2002, private communication), both the Lari models and the exponential models reproduce the profiles of low energy glitches, while the Lari model is the most appropriate for high energy glitches. In our simulation, however, we employed a one-component exponential model for simplicity.

Through the analysis of data from the far-infrared line mapper (FILM) onboard the Infrared Telescope in Space Mission (IRTS) (Murakami et al., 1996), we have classified glitches into four types, according to their profiles. In this simulation, we simplify the parameters which describe the shape of a glitch and assume that all glitches can be represented by the following equation:

$$S(t) = H_1\delta(t - t_0) + H_2 \exp\left[-\frac{t - t_0}{\tau}\right], \quad (2)$$

where $S(t)$ is the signal, H_1 and H_2 are the heights of the glitch for the delta function and the exponential component, respectively, t_0 is the event time of a glitch, and τ is the time constant. We assume that the heights of the glitches (H_1, H_2) follow a Gaussian distribution whose mean and dispersion are listed in Table 2. Table 2 also lists the other parameters of Eq. (2) for the four glitch types considered. Since we do not know exactly how the responsivity changes after a glitch, we assume that the responsivity remains constant irrespective of a glitch in this work. When more extensive data sets become available, we will also consider these response changes.

4. Results

4.1. Simulation data

Based upon our models and using laboratory data, we have simulated the transient response, the glitches and the crosstalk for the ASTRO-F/FIS simulation software. Fig. 2 shows the effect of the transient (a), crosstalk (b), and glitches (c and d). The transient causes a long tail along the scan direction. The effect of the crosstalk is to blur the image. The glitches appear as bright knots, or narrow and long bright lines if their strength is very high.

Actual observational data would be even more complicated, as these effects would occur together. In Fig. 3, we display the simulated images of an artificial sky covering $1^\circ \times 1^\circ$ area without (left panel) and with (right panel) detector characteristics. In these images, we use a power-law relation for the point source distribution with a power index $\gamma = 1.5$ and a normalization constant $N_0 = 10$ which corresponds to negligible source confusion (see Jeong et al., 2003 for details). The real task of data reduction is to remove these effects as effectively as possible. Below we discuss how we can eliminate such spurious effects.

4.2. Correction for the detector characteristics

In order to correct for the transient, we need to know the transient response function. We assume the same model of $r(t)$ used for the generation of data for the correction process. Since we know the incoming photon flux in the time sequence, we can estimate the leakage signal from the integration of the transient response by fitting the signal and finding the model parameters of the

Table 2
Parameters for four types of glitches

Type	Rate (s/glitch)	H_1 (mean, σ) (fA)	Cutoff for H_1 (fA)	H_2 (mean, σ) (fA)	Cutoff for H_2 (fA)	τ (s)
Type A (positive)	250	(10, 8.5)	>5	–	–	–
Type A (negative)	1000	(−6, 7)	<−5	–	–	–
Type B	1800	(10, 8.5)	>5	(15, 12)	>2	3
Type C	500	(10, 8.5)	>0	(−15, 12)	<−2	1
Type D	80,000	(200, 150)	>5	(35, 30)	>10	300

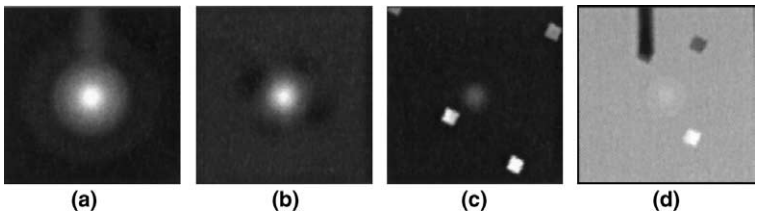

Fig. 2. Reconstructed image including transients (a), crosstalk (b) and glitches (c and d). After passing through the center of the source, we can see the tail of a signal (a). Panel (b) shows the residual image between the original image and the image including the crosstalk. Due to the high strength of the glitches, the shape of both the pixel and the glitch appear distinctively in the images (c and d).

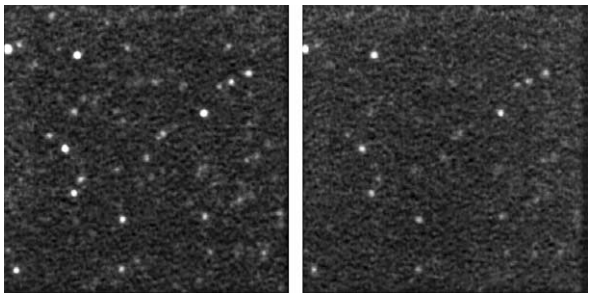

Fig. 3. Simulated $1^\circ \times 1^\circ$ images with many sources. The left panel is the image without the detector characteristics. The right panel is the image including the detector characteristics.

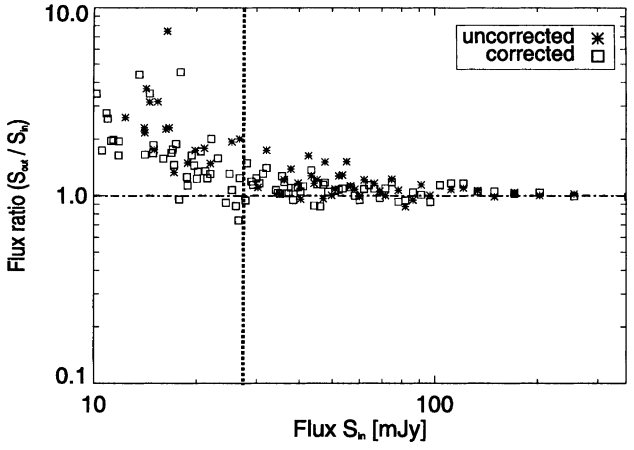

Fig. 4. Ratio of the output flux to the input flux. The asterisk symbols show the detected sources in the image including the detector characteristics, and the rectangles show the detected sources in the image after correcting for the detector characteristics. The vertical dotted line shows the estimated 5σ detection limit.

transient for each time sequence. We can therefore compensate for the signal affected by transient with these leakages for each time sequence.

Glitches and crosstalk are easier to recover. In the case of the glitches, we corrected them by replacing the corrupted signal by that of the other unglitched pixels passing through the same position. For the crosstalk effect, we simulate the crosstalk with a constant response for the surrounding pixels. Since we assumed that a constant fraction of a signal has leaked due to the crosstalk effect, we approximately correct it by collecting the same fraction of the signal from the surrounding pixels. For a more realistic correction, an iterative process should be applied. In practice, the correction accuracy of the transient and the crosstalk effects are determined by the consistency of the model parameters and the noise because the actual behavior of the detector may not exactly follow our simple model.

We have applied the above mentioned process to the simulated data shown in Fig. 3. We then carried out aperture photometry on both the image affected by the detector characteristics and the corrected image using the SExtractor software *v*2.0.0 (Bertin and Arnouts, 1996) in order to check the accuracy of our corrections. Fig. 4 shows the ratio of the output flux to the input flux, for the extracted and identified sources. For the purpose of calibrating the output flux, we used the five brightest input sources. Hence, the flux ratio of the bright sources is around 1.0 for the photometry on the image including the detector characteristics. At lower flux levels (below 20 mJy), the detected sources are limited by the photon and readout noise. In the case of the uncorrected image, the number of detected sources is 10% lower than those in the corrected image. In addition, the corrected image gives a much better result down to the detection limit.

5. Summary

We have carried out simulations including transients, glitches, and crosstalk effects for the detectors of ASTRO-F/FIS. We have employed simple models for these effects based on laboratory measurements. The corrections were applied to the simulated time series data, by adopting the same models which were used for generating the detector characteristics. Though we could accurately recover the input flux down to the detection limit, the actual behavior of the detector is affected by a combination of many detector characteristics that do not follow simple models. The change of the detector responsivity after a glitch is also an important issue for the data reduction process. We will investigate these issues more deeply in forthcoming works.

Acknowledgements

W.-S. Jeong, M. Kim, and S.H. Oh acknowledge the visiting fellowship by the BK21 Project of the Korean Government. This work was financially supported in part by the KOSEF Grant No. R14-2002-058-01000-0. The ASTRO-F project is managed and operated by the Institute of Space and Astronautical Science (ISAS), Japan, in collaboration with groups in universities and institutes in Japan as well as with Seoul National University, Korea. We thank André Fletcher in Korea Astronomy Observatory for help with editing this paper.

References

Bertin, E., Arnouts, S. SExtractor: software for source extraction. Astron. Astrophys. Suppl. Ser. 117, 393–404, 1996.

Jeong, W.-S., Pak, S., Lee, H.M., et al. Observing simulations of far-infrared surveyor: design overview and current status, in: Matsumoto, T., Shibai, H. (Eds.), Mid- and Far-Infrared Astronomy and Future Missions, ISAS Report SP14, ISAS, Sagamihara, Japan, pp. 297–304, 2000.

Jeong, W.-S., Pak, S., Lee, H.M., et al. ASTRO-F/FIS observing simulation: detection limits for point sources. P. Astron. Soc. Jpn. 55, 717–731, 2003.

Jeong, W.-S., Pak, S., Lee, H.M., et al. Simulations of cosmological observations with ASTRO-F/FIS. Adv. Space Res., this issue, 2004, doi:10.1016/j.asr.2003.04.040.

Kaneda, H., Okamura, Y., Nakagawa, T. Transient response of stressed Ge:Ga detector on-board ASTRO-F. Adv. Space Res. 30 (9), 2105–2110, 2002.

Kim, M., et al. Private communication, 2002.

Lari, C., Pozzi, F., Gruppioni, C., et al. A new method for ISOCAM data reduction – I. Application to the European Large Area ISO Survey Southern Field: method and results. Mon. Not. R. Astron. Soc. 325, 1173–1178, 2001.

Matsuura, S., Isozaki, Y., Shirahata, M., et al. Monolithic Ge:Ga two-dimensional array detector for FIS instrument on ASTRO-F, in: John, C.M. (Ed.), IR Space Telescopes and Instruments. Proc. of SPIE, vol. 4850, SPIE, Washington, USA, pp. 902–909, 2003.

Murakami, H., Freund, M., Ganga, K., et al. The IRTS (Infrared Telescope in Space) Mission. P. Astron. Soc. Japan 48, L41–L46, 1996.

Murakami, H. Japanese Infrared Survey Mission IRIS (ASTRO-F), in: Pierre, Y.B., James, B.B. (Eds.), Space Telescopes and Instruments V, Proc. of SPIE, vol. 3356., SPIE, Washington, USA, pp. 471–477, 1998.

Nakagawa, T. ASTRO-F survey as input catalogues for FIRST, in: Pilbratt, G.L., Cernicharo, J., Heras, A.M., Prusti, T., Harris, R. (Eds.), The Promise of the Herschel Space Observatory, ESA-SP 460, ESA Publications Division, Noordwijk, Holland, pp. 67–74, 2001.

Rieke, G.H. Detection of Light: From the Ultraviolet to the Submillimeter. Cambridge University Press, Cambridge, 1994.

Shibai, H. The ASTRO-F (IRIS) Mission, in: Harwit, M., Hauser, M.G. (Eds.), The Extragalactic Background and its Cosmological Implications, IAU Symp. No. 204, Astronomical Society of the Pacific, Michigan, USA, pp. 455–466, 2000.